Neurochemical Research (2024) 49:1655–1664
https://doi.org/10.1007/s11064-024-04101-3

ORIGINAL PAPER

Effect and Mechanism of LIN28 on Ferroptosis in Mg^{2+}-free Rat Hippocampal Neuron Model of Epilepsy

Xiaoke Wu[1,2] · Mengmeng Shi[1] · Yuan Chen[1] · Yajun Lian[1] · Shaokuan Fang[2] · Haifeng Zhang[1]

Received: 12 December 2022 / Revised: 30 December 2023 / Accepted: 3 January 2024 / Published online: 13 January 2024

Abstract

Studies have demonstrated that LIN28 is expressed in the CNS and may exert protective effects on neurons. However, it remains unknown whether LIN28 regulates ferroptosis in the context of epilepsy. In this study, we established an epilepsy model by culturing hippocampal neurons from rats in a magnesium-free (Mg^{2+}-free) medium. In Mg^{2+}-depleted conditions, hippocampal neurons exhibited reduced LIN28 expression, heightened miR-142-5p expression, decreased glutathione peroxidase (GPX) activity and expression, elevated levels of reactive oxygen species (ROS) and malondialdehyde (MDA), resulting in a significant decline in cell viability and an increase in ferroptosis. Conversely, overexpression of LIN28 reversed these trends in the mentioned indices. Altogether, this study reveals that LIN28 may exert neuroprotective effects by inhibiting the miR-142-5p expression and suppressing ferroptosis in hippocampal neurons induced by Mg^{2+}-free via increasing GPX4 expression.

Keywords LIN28 · Epilepsy · Hippocampal Neurons · GPX4 · Ferroptosis

Abbreviations

4-HNE	4-hydroxyrenenaldehyde
AD	Alzheimer's disease
ANOVA	Analysis of variance
BCA	Bicinchoninic acid
CCK-8	Cell Counting Kit-8
CNS	Central nervous system
GPX	Glutathione peroxidase
HD	Huntington's disease
mDA	Midbrain dopamine
MDA	Malondialdehyde
Mg^{2+}-free	Magnesium-free
miRNA	MicroRNA
NSE	Neuron specific enolase
PD	Parkinson's disease
RBP	RNA binding protein
ROS	Reactive oxygen species
SD	Standard deviation
SDS-PAGE	SDS-polyacrylamide gel electrophoresis
SN	Substantia nigra
TBST	Tris buffer solution tween
TEM	Transmission electron microscope

Introduction

Epilepsy is a prevalent neurological disorder that affects approximately 50 million people worldwide [1]. Approximately 30% of epilepsy patients show resistance to antiepilepsy drugs, and temporal lobe epilepsy is a typical representative of them [2]. Hippocampal neuronal loss is the main pathological feature of epilepsy and involves multiple cell death modalities such as apoptosis, necrosis, autophagy, pyroptosis, and ferroptosis [3]. Ferroptosis is a new type of programmed cell death first proposed in 2012, and several studies have demonstrated that role of ferroptosis in epilepsy [3–6]. Therefore, strategies for preventing neuronal ferroptosis can potentially treat epilepsy.

Xiaoke Wu and Mengmeng Shi contributed equally to this work.

✉ Shaokuan Fang
jluneu@163.com

✉ Haifeng Zhang
zhf840317@163.com

[1] Department of Neurology, The First Affiliated Hospital of Zhengzhou University, Zhengzhou, Henan 450052, China

[2] Department of Neurology, Neuroscience Centre, The First Hospital of Jilin University, Changchun, Jilin 130021, China

LIN28 is an evolutionarily highly conserved RNA binding protein (RBP) that plays an essential role in embryogenesis, skeletal muscle formation, germ cell development, neuronal stem cell differentiation, and glucose metabolism. Recent studies have found that LIN28 is likely to play an important role in CNS diseases [7–9]. However, its role in epilepsy and regulatory mechanisms are not fully understood.

MicroRNAs (miRNAs) are single-stranded non-coding RNAs with lengths in the range of 19–23 nucleotides that modulate cell development, immune response, proliferation, apoptosis, differentiation, and many other life processes [10]. In our previous study, we found that a miR-142-5p antagonist inhibited neuronal death, attenuated hippocampal damage in temporal lobe epileptic mice, improved mitochondrial function, increased mitochondrial membrane potential, inhibited ROS production, and attenuated oxygen-glucose deprivation-induced neuronal damage [11, 12]. Other studies have reported that LIN28 reduces its expression by binding to pre-let-7 during embryonic differentiation. During neuronal differentiation in the mouse embryonic carcinoma cell line P19, LIN28 inhibits miR-9 biogenesis and suppresses neuronal differentiation by binding to pre-miR-9 [13, 14]. Bioinformatics tools, it was predicted that LIN28 can bind to the 'GGAG' motif of pre-miRNA-142 to regulate miR-142-5p formation. Is it possible for LIN28 to influence the production of miR-142-5p in a similar manner, subsequently regulating the downstream ferroptosis process?

Ferroptosis as a non-apoptotic form of cell death that is characterized by iron-dependent lipid peroxidation and metabolic inhibition. GPX4 has been shown to be a negative regulator of ferroptosis, and inhibition of GPX4 function results in lipid peroxidation and leads to ferroptosis [15]. Previously, melatonin was found to improve ischemic-hypoxic brain injury by regulating hippocampal neuronal ferroptosis via GPX4 signaling [16]. Therefore, we postulated whether LIN28 may regulate miR-142-5p levels and exert neuroprotective effects by controlling hippocampal neuronal ferroptosis via GPX4 signaling.

To explore the roles of LIN28, miR-142-5p, GPX4, ferroptosis, and epileptogenesis, we investigated the LIN28/miR-142-5p/GPX4 signaling pathway and its effect on ferroptosis in neuronal cells at the cellular level.

Methods

Bioinformatics Prediction

The effects of LIN28 on miR-142-5p were explored on the miRBase bioinformatics database.

Isolation of Primary Hippocampal Neurons in Newborn Rats

Newborn SD rats obtained from the Animal Experimental Center of Zhengzhou University were disinfected with 75% alcohol and decapitated within 24 h of birth. Brain tissue was excised under aseptic conditions, and hippocampal tissue was isolated and minced. The tissue samples were then digested by treatment with 0.125% trypsin at 37℃ for 20–25 min. The digested samples were filtered using a 200-mesh sieve, and then inoculated in a neurobasal medium containing 2% B27, and incubated at 37℃ in a 5% CO_2 sterile cell culture chamber (Lishen, Shanghai, China). After three days, cytidine was added to 5 μm in cell culture medium, the medium was changed every three days, and hippocampal neurons were cultured for subsequent experiments. The cell morphology of hippocampal neurons was first observed under an inverted phase contrast microscope (OLYMPUS, Japan), and the anti-neuron specific enolase (NSE) (Abcam, USA) was utilized to identify the purity of hippocampal neuron cells through immunofluorescence detection.

Experimental Design and Establishment of Epileptiform Discharge Model

When the cell density reached a confluence of about 60–70%, lentiviral transfection was performed. All lentiviruses were purchased from GeneChem (Shanghai, China). The primary hippocampal neurons were randomly divided into four groups: (1) control group: After incubation for 10 days, neurons were treated with normal medium (0.002 mM glycine, 1mM $MgCl_2$, 2 mM $CaCl_2$, 2.5 mM KCl, 10 mM glucose, 10 mM HEPES, 145 mM NaCl dissolved in sterile water, pH 7.4) for 3 h, and cultured in serum-free medium; (2) No Mg^{2+} group: After incubation for 10 days, then the medium was replaced with a Mg^{2+}-free physiological solution (normal medium without magnesium) and incubated for 3 h, and then normal medium culture was resumed [17, 18]; (3) No Mg^{2+}+Vector group: After the neurons were cultured for 6 days, the lentiviral vector was diluted in serum-free medium to treat neurons for 24 h and cultivated with normal medium for 24 h. Finally, on the 10th day, the neurons in the Mg^{2+}-free group were treated with Mg^{2+}-free medium for 3 h, followed by culture in a serum-free medium for 24 h; (4) No Mg^{2+}+ LV-LIN28 group (LIN28 overexpression): Lentivirus-LIN28 was diluted in a serum-free medium and applied to treat neurons for 24 h after 6 days of incubation, and the subsequent treatment was the same as that in the NC group (Table 1). After treatment with normal cell extract or Mg^{2+}-free extract for 3 h, the cells were cultured with

Table 1 Culturing flow of hippocampal neurons in each group

Group	Lentiviral transfection	Modeling
control group	normal culture	Normal solution treatment for 3 h
No Mg^{2+}group	normal culture	Mg^{2+}-free solution treatment for 3 h
No Mg^{2+}+Vector group	transfected with lentivirus-vector	Mg^{2+}-free solution treatment for 3 h
No Mg^{2+}+ LV-LIN28 group	transfected with lentivirus-LIN28	Mg^{2+}-free solution treatment for 3 h

Table 2 The primer sequences for QPCR

Gene	Sequences
GAPDH-F	GACAACTTTGGCATCGTGGA
GAPDH-R	ATGCAGGGATGTTCTGG
LIN28-F	TGGTGTGTTCTGTATTGGGAGT
LIN28-R	AGTTGTAGCACCTGTCTCCTTT
GPX4-F	CCAAAGTCCTAGGAAAACGCCC
GPX4-R	GGGCATCGTCCCCATTTACA
U6-F	CGCAAGGATGACACGCAAAT
U6-R	GTGCAGGGTCCGAGGTATTC
miR-142-5p-F	GCCGCCATAAAGTAGAAAGC
miR-142-5p-R	GGTGCAGGGTCCGAGGTAT

maintenance culture medium was continued for 24 h for further experiments.

QPCR to Detect the Expression of LIN28, miR-142-5p, GPX4

Total RNAs were extracted from hippocampal neurons using the RNAiso Plus reagent following the manufacturer's instructions (Takala, China). Subsequently, RNA was reverse transcribed to cDNA using a reverse transcription kit (Takala, China) and subsequently subjected to quantitative polymerase chain reaction (QPCR) using QPCR Master Mix (Vazyme, China) according to the manufacturer's instructions. All data were analyzed and normalized to the expression of GAPDH or U6, and the primer sequences as follows (Table 2):

Western Blot to Detect the Expression of LIN28, GPX4

Total protein was extracted from the cells by using RIPA lysis buffer (Epizyme, Shanghai). The proteins were quantified using the bicinchoninic acid (BCA) Protein Analysis kit (Solarbio, Beijing). Equal amounts of protein were loaded into a polyacrylamide gel and separated by SDS-polyacrylamide gel electrophoresis (SDS-PAGE). They were then electro-transferred to a PVDF membrane (Millipore, USA). The membrane was blocked with 5% BSA on tris buffer solution tween (TBST) and incubated with primary antibodies against LIN28 (1:1000, CST, USA), GPX4 (1:1000, CST, USA), andβ-actin (1:2000, CST, USA) at 4℃ overnight and then hybridized with a secondary antibody (rabbit antibody, 1:5000, Proteintech) at room temperature for 1 h. β-actin was used as an internal control for either total cellular or cytosolic proteins. Finally, the intensity of the bands was observed using the ECL kit (Sea Biotech, China).

Lipid Peroxidation Analysis

Centrifuging at 140 g for 5 min to ollecte each group of hippocampal neurons. BODIPY 581/591 C11 (Thermo, USA) at a concentration of 5μmol/L was added to the cells, mixed and incubated for 30 min in an incubator at 37℃. The cells were then washed with PBS three times, resuspended in 0.5 mL PBS for flow cytometry assay (Suzhou Purification, Suzhou).

The neuronal cells from each group were collected and ultrasonically crushed under ice bath conditions. A BCA protein concentration assay kit (Wanleibio, China) was used to quantify the protein in the supernatant. Then the MDA content of each group was assessed using an MDA reagent (Wanleibio, China). The GPX activity of the samples was determined using a GSH-Px kit (Wanleibio, China).

Ferroptosis and Analysis of Intracellular Iron Deposition

The mitochondrial morphology and neurons were observed with the transmission electron microscopy (TEM) and then centrifuged (4℃, 1000 g, 5 min). The cells were then counted and centrifuged to obtain supernatants (4℃, 16,000 g, 10 min). Intracellular iron was detected using iron assay kit (Abcom, Britain) following the manufacturer's instructions.

CCK-8 Assay to Detect Neuronal Viability

After transfection for 48 h, the cells were switched to a Mg^{2+}-free physiological solution and cultured for an additional 3 h, and then subject to the CCK-8 assay. Subsequently, 10μL of CCK-8 (Wanleibio, China) was introduced into each well and incubated at 37℃ with 5% CO_2 for 2 h. The OD value at 450 nm was measured using an enzyme marker (BIOTEK, USA).

Statistical Analysis Method

The statistical analysis was processed using GraphPad Priam 8.0 statistical software. Measurement data were shown as mean ± standard deviation (SD). And one-way analysis of variance (ANOVA) followed by Tukey's multiple

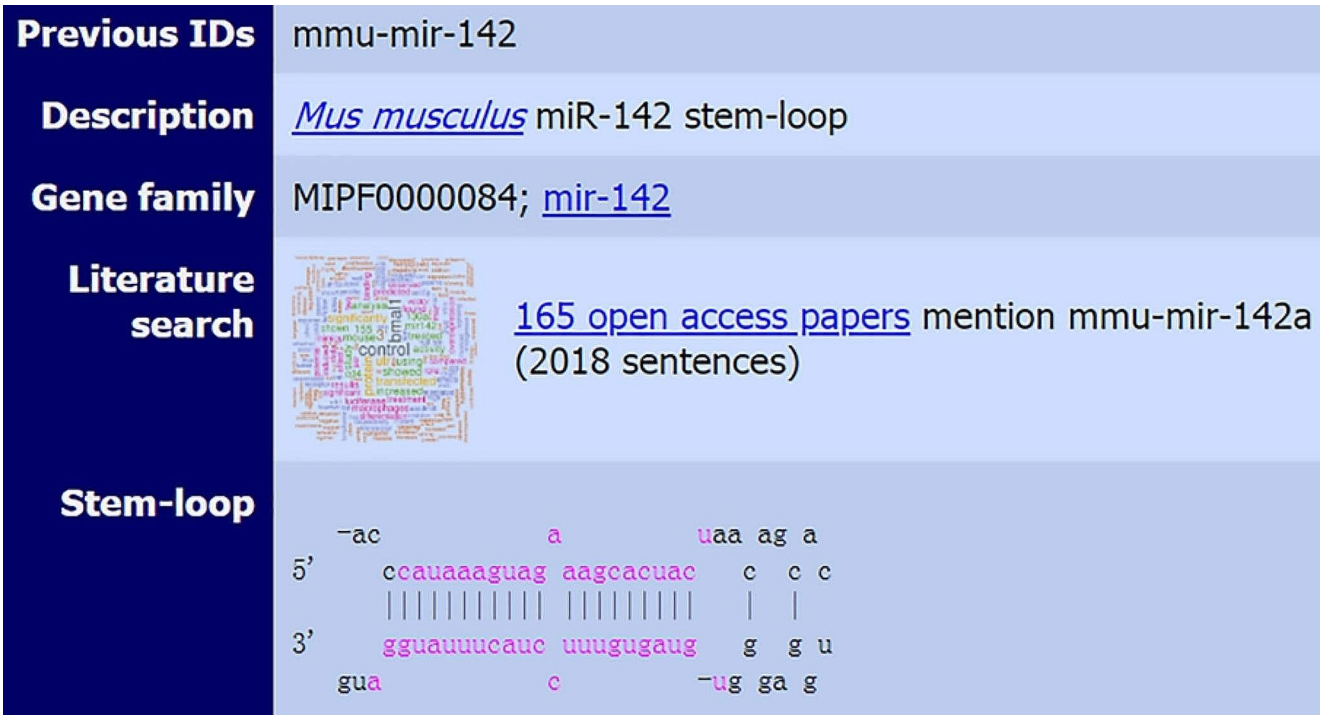

Fig. 1 The miR-142-5p precursor sequence

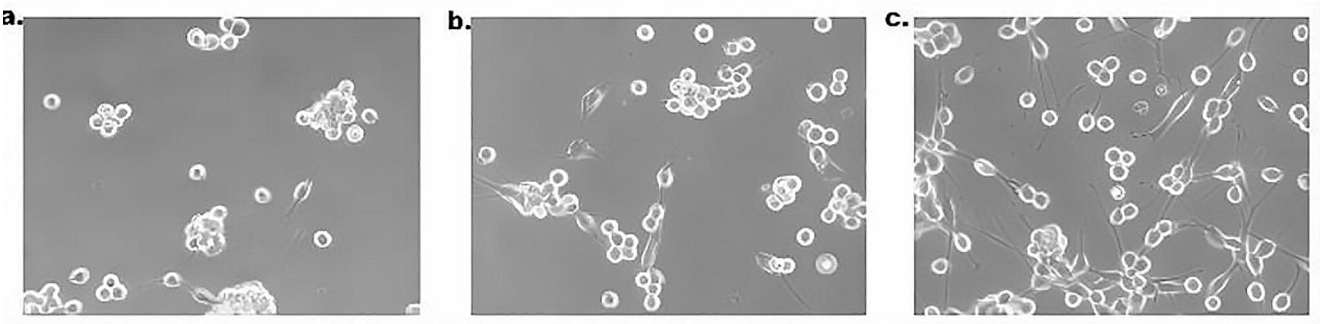

Fig. 2 Neuronal morphology was observed under microscope (magnification, ×400). **a** Hippocampal neurons were cultured for 3 days. **b** Hippocampal neurons were cultured for 5 days. **c** Hippocampal neurons were cultured for 9 days

comparisons test for comparison among groups. $P < 0.5$ was considered statistically significant.

Results

LIN28 Binds to miR-142-5p Precursor pre-miRNA and Induces miRNA Degradation

Analysis of the miRBase bioinformatics database revealed that pre-miR-142 contains a "GGAG" sequence in its terminal loop (Fig. 1). Further literature review revealed that LIN28 could bind to the 'GGAG' motif of pre-miRNA to induce miRNA degradation [19]. The results predicted that LIN28 may promote miRNA degradation by binding to the 'GGAG' sequence of pre-miRNA.

Isolation of Neonatal Rat Hippocampal Neurons

Hippocampal neurons were isolated from neonatal SD rats within 24 h. The cells were incubated and the cell morphology was recorded using microscope, and two to three small protrusions were observed after 3 days of culture. After 5 days of culture, the neurons expanded into shuttle-shaped, high-temperature cone-shaped and polygonal. The cells were cultured for 9 days, and were observed to be enlarged and full, surrounded by a halo, and the protrusions were in contact with each other, forming a complex neural network (Fig. 2). Immunofluorescence staining was performed to

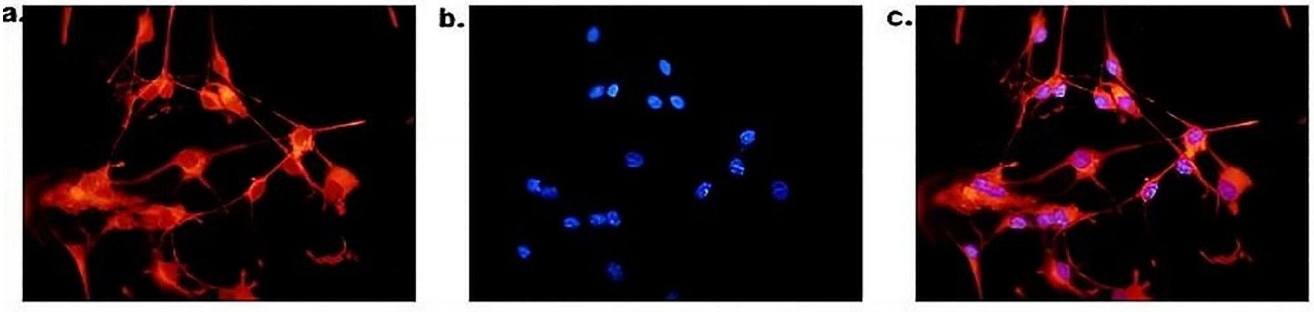

Fig. 3 The neuronal marker neurofilament (neurofilament) was visualized by immunofluorescence staining and the cell purity was identified (magnification,×400). **a** Neurofilament. **b** DAPI. **c** Merge

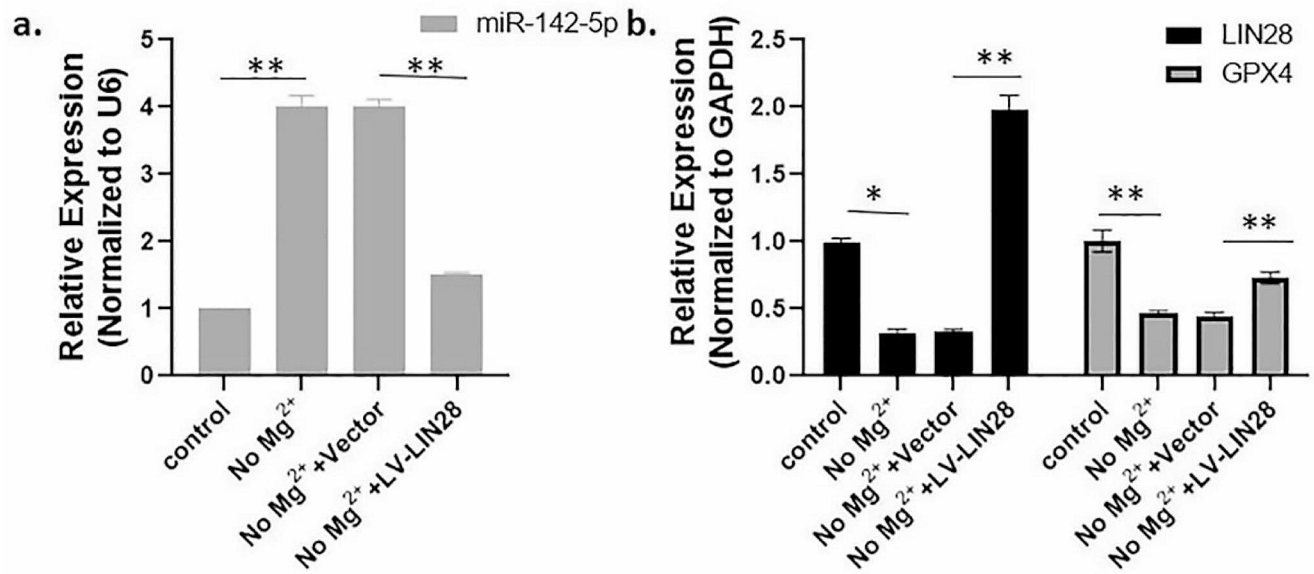

Fig. 4 Target molecular expression was determined by Real-time PCR. **a** Expression of miR-142-5p in the group of control, No Mg^{2+}, No Mg^{2+}+Vector, and No Mg^{2+}+LV-LIN28 compared with U6. **b** Lin28 and GPX4 expression in the group of control, No Mg^{2+}, No Mg^{2+}+Vector, and No Mg^{2+}+LV-LIN28 compared with GAPDH. Comparing with the control group, ** $P<0.01$, * $P<0.05$; comparing with the No Mg^{2+}+Vector group, ** $P<0.01$, * $P<0.05$

observe neurofilament, a neuronal marker, and to identify the purity of the cells. The results showed that neuronal purity was over 95% of 300 cells (Fig. 3).

LIN28 Expression in the Epileptiform Discharge Model

Hippocampal neuronal cells were transfected with LIN28 overexpression lentivirus, and a spontaneous epileptiform discharge model was established using a Mg^{2+}-free physiological solution. Real-time PCR was performed to detect the expression of LIN28, miR-142-5p, GPX4, whereas the expression of LIN28 and GPX4 proteins was determined by Western blot. The results showed that compared with the control group, the No Mg^{2+} group had significantly lower expression level of LIN28 and GPX4 and significantly higher expression of miR-142-5p. Compared with the Vector group, the protein level of GPX4 in the LV-LIN28 group was significantly higher, and the manifestation of miR-142-5p was significantly lower (Figs. 4 and 5).

ROS, MDA Content and GPX Activity in the Epileptic Discharge Model

The ROS and MDA contents were significantly increased and GPX activity was significantly decreased in the No Mg2 + group relative to the control group, and the ROS and MDA contents were decreased significantly and the GPX activity was markedly higher in the LV-LIN28 group relative to the Vector group. (Figures 6 and 7).

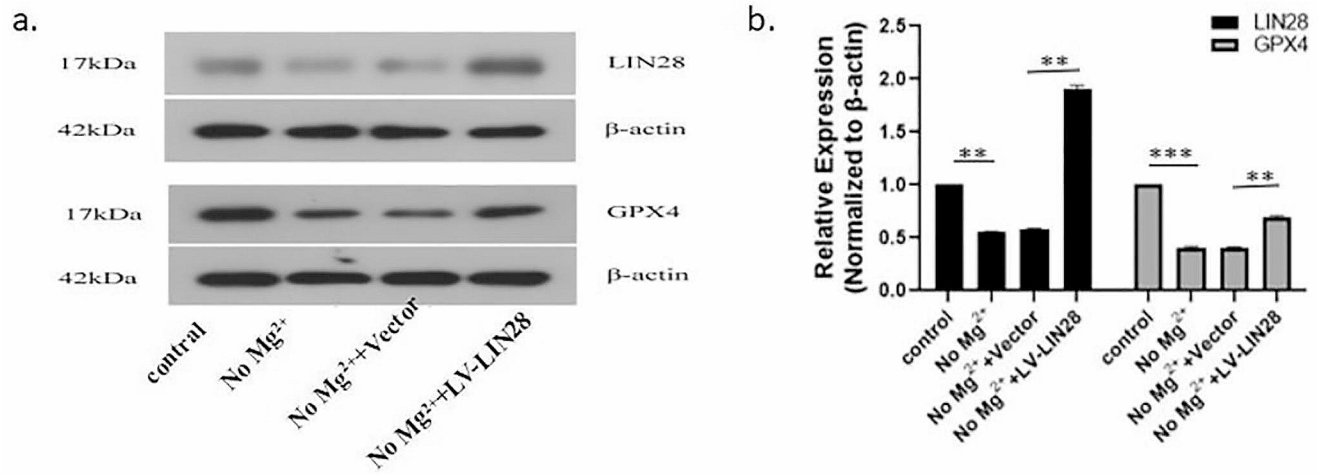

Fig. 5 Western blot analysis for protein expression.β-actin is used as an internal reference. **a** Expression of Lin28 and GPX4 in the group of control, No Mg^{2+}, No Mg^{2+}+Vector, and No Mg^{2+}+LV-LIN28. **b** Lin28 and GPX4 expression in the control, No Mg^{2+}, No Mg^{2+}+Vector, and No Mg^{2+}+LV-LIN28 groups. Comparing with the control group, ** $P<0.01$, * $P<0.05$; comparing with the No Mg^{2+}+Vector group, ***$P<0.001$, ** $P<0.01$, * $P<0.05$

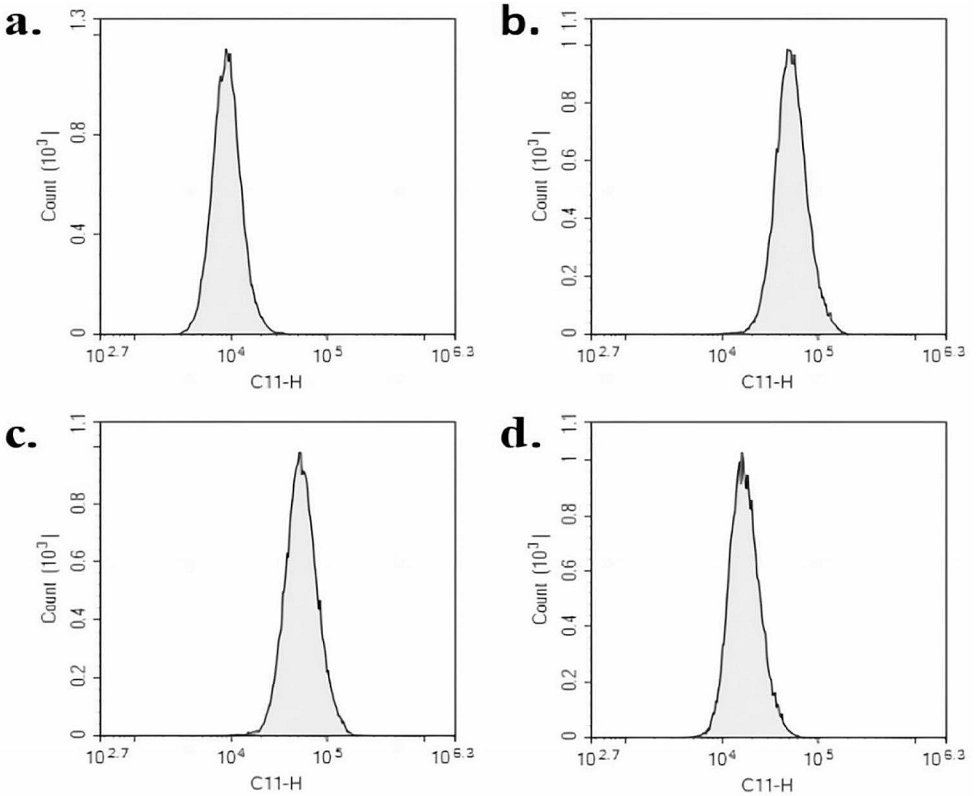

Fig. 6 Flow detection of the ROS. The **a, b, c, d** is the group of control, No Mg^{2+}, No Mg^{2+} + Vector, and and No Mg^{2+} + LV-LIN28 respectively

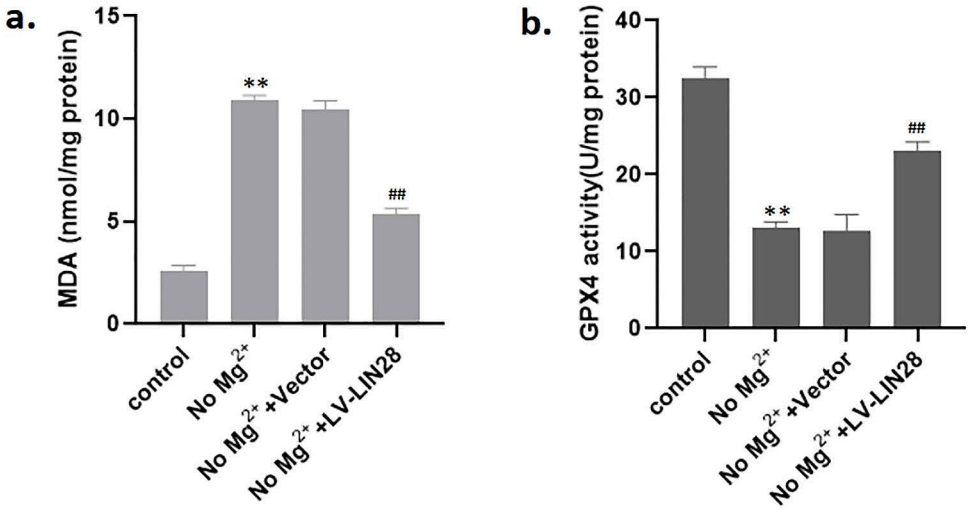

Fig. 7 Kit detection for MDA and GPX. **a** Detection of the MDA concentration. **b** Detection of the GPX activity. For the control group, ** $P < 0.01$, and for the No Mg^{2+}+Vector group, $^{\#\#}P < 0.01$

Assessment of LIN28 Effect on Ferroptosis

The results showed that compared with the control group, the No Mg^{2+} group cells had significantly smaller mitochondria and significantly increased iron deposition. Analysis of CCK-8 assay revealed that cell viability was decreased. Compared with the Vector group, the LV-LIN28 group showed substantially larger mitochondria, reduced iron deposition, and considerably higher cell viability (Figs. 8 and 9).

Discussion

Hippocampal neuronal loss is a major pathological feature of temporal lobe epilepsy, involving various patterns of cell death, including apoptosis, necrosis, autophagy, and pyroptosis. Ferroptosis is a new type of programmed cell death first discovered in 2012, characterized by reduced antioxidant capacity and massive accumulation of lipid oxidation in cells, mitochondrial contraction, reduced or disappearance of cristae, altered membrane potential, and mitochondrial membrane rupture [3]. The researchers believe that decreased ferritin promotes neuronal death in Parkinson's disease (PD), Alzheimer's disease (AD), and Huntington's disease (HD) [20]. Recent studies have demonstrated the role of ferroptosis in epilepsy. Data shows that in the ferric chloride ($FeCl_3$) -induced traumatic epilepsy model, baicalein reduces the number and average duration of seizures by inhibiting ferroptosis in mice. The ferroptosis inhibitor ferrostatin-1 can significantly alleviate the IV and pilocarpine-induced episodes in mice and decrease the amount of lipid peroxide 4-hydroxyrenenaldehyde (4-HNE) and MDA in the hippocampus. Furthermore, ferrostatin-1 prevented alginate-induced temporal lobe epilepsy, reduced hippocampal neuronal loss and restored cognitive function in rats [4–6]. Altogether, these findings indicate that there is abnormal iron metabolism and iron-mediated oxidative damage during the pathogenesis of epilepsy, and strategies for preventing neuronal ferroptosis can effectively treat epilepsy.

Ferroptosis is regulated by many factors, such as GPX4, lipid synthesis, iron metabolism, methyl hydroxacid and so on [15, 21–23]. Decreased activity of GPX4 induced ferroptosis in osteosarcoma cells, enhancing its sensitivity to cisplatin. Melatonin regulates hippocampal neuronal ferroptosis via GPX4 and improves ischemic hypoxic brain injury. Seratrodast inhibited ferroptosis by increasing GPX4 expression level. Overall, these findings suggest that GPX4 plays a crucial role as a negative regulator of cell ferroptosis [16, 24, 25]. In this study, it was observed that the expression of GPX4 significantly decreased in neurons exhibiting spontaneous epileptic discharges. This decrease was accompanied by elevated levels of ROS and MDA, a reduction in mitochondrial volume, and increased intracellular iron deposition. Collectively, these results indicate that ferroptosis occurs in hippocampal neurons during epileptogenesis and can be reversed following LIN28 overexpression.

LIN28, also known as LIN28a in mammals, is a highly conserved RBP involved in embryogenesis, skeletal muscle formation, germ cell development, neuronal stem cell differentiation, and glucose metabolism [26]. Recently, it has been found that LIN28a is also expressed in the CNS, where it promotes the proliferation of neural progenitors and exerts a pro-survival effect on primary cortical neurons [7]. Fatima et al.'s study also demonstrated that upregulated Lin28a promoted long-distance regeneration of corticospinal axons and the optic nerve in mouse models of optic nerve and spinal cord injury [8]. This suggests that LIN28 could be a crucial molecular target for treating CNS injuries. In addition, LIN28 conditional knockout mice showed mDA neuronal degeneration in the SN and PD-related behavioral defects,

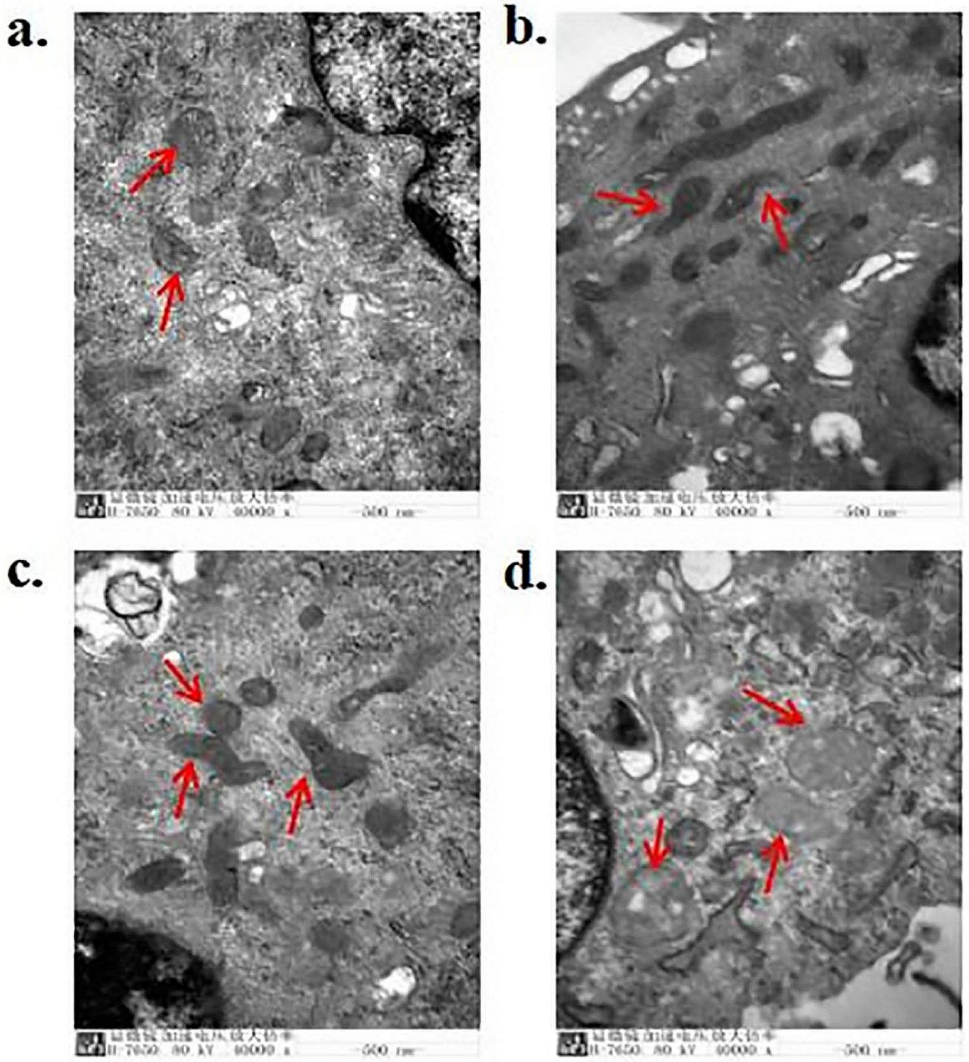

Fig. 8 Mitochondrial morphology was visualized by TEM (magnification, ×40,000; scale bar, 500 nm). **a** The group of control. **b** The group of No Mg^{2+}. **c** The group of No Mg^{2+}+Vector. **d** The group of No Mg^{2+}+LV-LIN28. Comparing with the control group, mitochondria were significantly smaller in the No Mg^{2+} group; mitochondrial volume was significantly increased in neurons in the No Mg^{2+}+LV-LIN28 group as compared to the No Mg^{2+}+Vector group

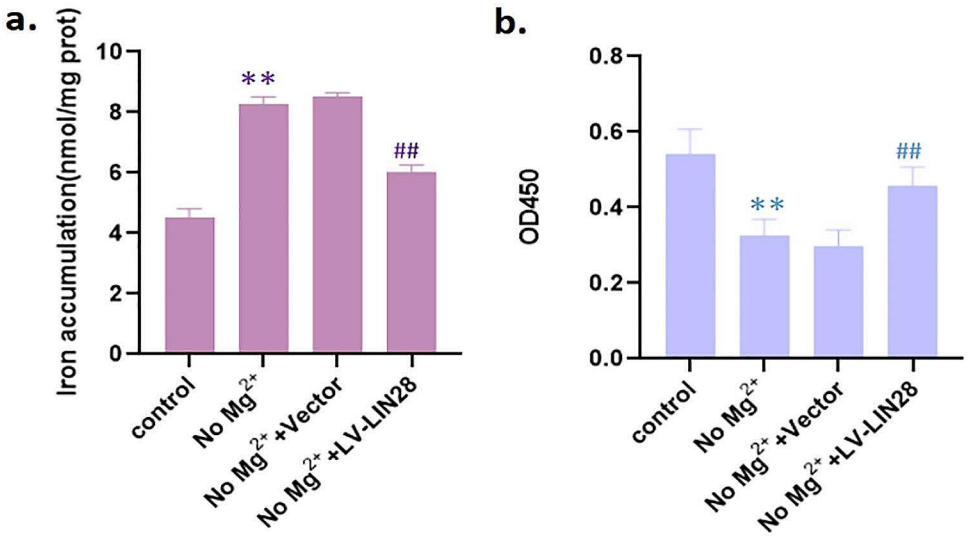

Fig. 9 Detection of iron accumulation and CCK-8. **a** Iron accumulation was detected by the kits. **b** Cell viability was measured by CCK-8. For comparison with the control group, $^{**}P < 0.01$; and when compared with the No Mg^{2+}+Vector group, $^{\#\#}P < 0.01$

and LIN28a upregulation enhanced central neuronal regeneration and promoted the therapeutic effects of neural stem cells on PD [9]. Together, these findings indicate that LIN28 has an essential role in CNS diseases, but its function in epileptic disorders has not been clarified. In this study, we found that the expression of LIN28 was significantly reduced in the epileptiform discharge model established by a Mg^{2+}-free solution. This significantly inhibited the occurrence of cell ferroptosis in hippocampal neurons and promoted cell viability.

MiRNA is a single-stranded non-coding RNA with lengths in the range of 19–23 nucleotides which participate in cell development, immune response, proliferation, apoptosis, differentiation, and other life processes by inhibiting mRNA translation and binding to other functional proteins [10]. During neuronal differentiation in the mouse embryonic cancer cell line P19, LIN28 inhibits miR-9 biogenesis by binding to pre-miR-9 which ultimately suppresses neuronal differentiation [14]. LIN28 can attach to the 'GGAG' motif of the pre-miRNA to induce miRNA degradation [19]. Together with the bioinformatics prediction results, we speculated that LIN28 might inhibit the formation of the mature body miR-142-5p by binding to pre-miR-142. Our previous study demonstrated that miR-142-5p antagonists inhibited neuronal death, attenuated hippocampal damage, improved mitochondrial membrane potential, inhibited ROS generation, and enhanced mitochondrial function in mice with temporal lobe epilepsy [11]. In this study, experimental results revealed that LIN28 overexpression reduced miR-142-5p production, and enhanced the antioxidant enzyme GPX4 expression thereby reversing the ferroptosis in Mg^{2+}-free epileptogenic rats and exerted neuroprotective effects.

In conclusion, we speculate that LIN28 can bind to pre-miR-142 and prevent the formation of mature miR-142-5p. This further suppresses ferroptosis in hippocampal neurons, and ultimately inhibits epileptogenesis via GPX4 signaling. Further in vivo experiments are needed to validate our hypothesis and reveal new targets for developing therapeutic strategies for epilepsy.

Acknowledgements We are particularly grateful to the supportion provided by the First Affiliated Hospital of Zhengzhou University (Zhengzhou, China).

Author Contributions HFZ, YJL, SKF provided direction and guidance throughout the preparation of this manuscript, and revised the manuscript. XKW, MMS performed the experiments, collected and prepared the related papers. XKW, HFZ wrote the manuscript. All authors approved the final manuscript.

Funding This study was supported by The National Natural Science Foundation of China (No.81701271, 81771397) and The China Association against Epilepsy Foundation (No.UCB-2023-056).

Declarations

Ethical Statement This study were approved by Ethics Committee of The First Affiliated Hospital of Zhengzhou University (2022-KY-0271).

Competing Interests The authors declare no competing interests.

References

1. Li Q et al (2019) Targeting gap junction in epilepsy: perspectives and challenges. Biomed Pharmacother 109:57–65
2. Fiest KM et al (2017) Prevalence and incidence of epilepsy: a systematic review and meta-analysis of international studies. Neurology 88(3):296–303
3. Dixon SJ et al (2012) Ferroptosis: an iron-dependent form of non-apoptotic cell death. Cell 149(5):1060–1072
4. Li Q et al (2019) Baicalein exerts neuroprotective effects in FeCl(3)-induced posttraumatic epileptic seizures via suppressing ferroptosis. Front Pharmacol 10:638
5. Mao XY, Zhou HH, Jin WL (2019) Ferroptosis induction in pentylenetetrazole kindling and pilocarpine-induced epileptic seizures in mice. Front Neurosci 13:721
6. Ye Q et al (2019) Inhibition of ferroptosis processes ameliorates cognitive impairment in kainic acid-induced temporal lobe epilepsy in rats. Am J Transl Res 11(2):875–884
7. Bhuiyan MI et al (2013) Expression of exogenous LIN28 contributes to proliferation and survival of mouse primary cortical neurons in vitro. Neuroscience 248:448–458
8. Nathan FM et al (2020) Upregulating Lin28a promotes axon regeneration in adult mice with optic nerve and spinal cord injury. Mol Ther 28(8):1902–1917
9. Chang MY et al (2019) LIN28A loss of function is associated with Parkinson's disease pathogenesis. Embo j 38(24):e101196
10. Pasquinelli AE (2012) MicroRNAs and their targets: recognition, regulation and an emerging reciprocal relationship. Nat Rev Genet 13(4):271–282
11. Zhang H et al (2020) Antagomirs targeting mir-142-5p attenuate pilocarpine-induced status epilepticus in mice. Exp Cell Res 393(2):112089
12. Wang N et al (2017) Down-regulation of microRNA-142-5p attenuates oxygen-glucose deprivation and reoxygenation-induced neuron injury through up-regulating Nrf2/ARE signaling pathway. Biomed Pharmacother 89:1187–1195
13. Shyh-Chang N, Daley GQ (2013) Lin28: primal regulator of growth and metabolism in stem cells. Cell Stem Cell 12(4):395–406
14. Nowak JS et al (2014) Lin28a regulates neuronal differentiation and controls miR-9 production. Nat Commun 5:3687
15. Yang WS et al (2014) Regulation of ferroptotic cancer cell death by GPX4. Cell 156(1–2):317–331
16. Gou Z et al (2020) Melatonin improves hypoxic-ischemic brain damage through the Akt/Nrf2/Gpx4 signaling pathway. Brain Res Bull 163:40–48
17. Zhang Y et al (2023) FUNDC1 mediated mitophagy in epileptic hippocampal neuronal injury induced by magnesium-free fluid. Neurochem Res 48(1):284–294
18. Yu X et al (2023) Activating transcription factor 4-mediated mitochondrial unfolded protein response alleviates hippocampal neuronal damage in an in vitro model of epileptiform discharges. Neurochem Res 48(7):2253–2264

19. Wilbert ML et al (2012) LIN28 binds messenger RNAs at GGAGA motifs and regulates splicing factor abundance. Mol Cell 48(2):195–206
20. Guiney SJ et al (2017) Ferroptosis and cell death mechanisms in Parkinson's disease. Neurochem Int 104:34–48
21. Gao M, Jiang X (2018) To eat or not to eat-the metabolic flavor of ferroptosis. Curr Opin Cell Biol 51:58–64
22. Hassannia B, Vandenabeele P, Vanden Berghe T (2019) Targeting ferroptosis to iron out cancer. Cancer Cell 35(6):830–849
23. Shimada K et al (2016) Global survey of cell death mechanisms reveals metabolic regulation of ferroptosis. Nat Chem Biol 12(7):497–503
24. Guo C et al (2020) Exosomal noncoding RNAs and tumor drug resistanceexosomal noncoding rnas on tumor drug resistance. Cancer Res 80(20):4307–4313
25. Kahn-Kirby AH et al (2019) Targeting ferroptosis: a novel therapeutic strategy for the treatment of mitochondrial disease-related epilepsy. PLoS ONE 14(3):e0214250
26. Mayr F, Heinemann U (2013) Mechanisms of Lin28-mediated miRNA and mRNA regulation—a structural and functional perspective. Int J Mol Sci 14(8):16532–16553